Mini-review for Molecular Pharmacology

New insights for drug design from the X-ray crystallographic structures of GPCRs

Kenneth A. Jacobson and Stefano Costanzi

Molecular Recognition Section, Laboratory of Bioorganic Chemistry (KAJ), and Laboratory of
Biological Modeling (SC), National Institutes of Diabetes and Digestive and Kidney Diseases,
National Institutes of Health, Bethesda, Maryland 20892.

Running title: Drug design from GPCR crystallographic structures

Corresponding author:

Kenneth A. Jacobson, Ph.D., Laboratory of Bioorganic Chemistry, National Institutes of
Diabetes and Digestive and Kidney Diseases, NIH, Bldg. 8A, Rm. B1A-19, Bethesda, MD
20892-0810, USA

Email: kajacobs@helix.nih.gov.

Phone: 301-496-9024.

Fax: 301-480-8422.

Text pages: 11

Number of tables: 1

Number of figures: 6

Number of references: 92

Number of words in Abstract: 227

Number of words in Introduction: 632

Number of words in Discussion: n/a

Abbreviations: BPM, biophysical mapping; BRIL, thermostabilized apocytochrome b_{562}RIL;
CVX15, cyclic disulfide of H-Arg-Arg-Nal-Cys-Tye-Gln-Lys-D-Pro-Pro-Tyr-Arg-Cit-Cys-Arg-
Gly- D-Pro-OH; DREADD, designer receptors exclusively activated by designer drugs; EL,
extracellular loop; IL, intracellular loop; IT1t, 6-dimethyl-5H,6H-imidazo[2,1-b][1,3]thiazol-3-
yl}methyl)sulfanyl]methanimidamide; ML056, (R)-3-amino-(3-hexylphenylamino)-4-
oxobutylphosphonic acid; SPR, surface plasmon resonance; StaR, thermostabilized form of a
GPCR, TM, transmembrane helix; RASSL, receptor activated solely by synthetic ligands; UK-
432097, 2-(3-[1-(pyridin-2-yl)piperidin-4-yl]ureido)ethyl-6-N-(2,2-diphenylethyl)-5′-N-
ethylcarboxamidoadenosine-2-carboxamide; ZM241385, 4-(2-(7-amino-2-(furan-2-yl)-
[1,2,4]triazolo[1,5-a][1,3,5]triazin-5-ylamino)ethyl)phenol.

Abstract

Methodological advances in X-ray crystallography have made possible the recent solution of X-ray structures of pharmaceutically important G protein-coupled receptors (GPCRs), including receptors for biogenic amines, peptides, a nucleoside and a sphingolipid. These high-resolution structures have greatly increased our understanding of ligand recognition and receptor activation. Conformational changes associated with activation common to several receptors entail outward movements of the intracellular side of transmembrane helix 6 (TM6) and movements of TM5 toward TM6. Movements associated with specific agonists or receptors have also been described, e.g. extracellular loop 3 (EL3) in the A_{2A} adenosine receptor. The binding sites of different receptors partly overlap but differ significantly in ligand orientation, depth and breadth of contact areas in TM regions, and the involvement of the ELs. A current challenge is how to utilize this structural information for the rational design of novel potent and selective ligands. For example, new chemotypes were discovered as antagonists of various GPCRs by subjecting chemical libraries to *in silico* docking in the X-ray structures. The vast majority of GPCR structures and their ligand complexes are still unsolved, and no structures are known outside of Family A GPCRs. Molecular modeling, informed by supporting information from site-directed mutagenesis and structure activity relationships, has been validated as a useful tool to extend structural insights to related GPCRs and to analyze docking of other ligands in already crystallized GPCRs.

Introduction

In the past five years, progress in the structure-based design of ligands for G protein-coupled receptors (GPCRs) has greatly accelerated. The major contributing factor has been the elucidation of X-ray crystallographic structures of high resolution for various drug-relevant GPCRs, initially in the inactive antagonist-bound forms and more recently in agonist-bound forms. The initial breakthrough were the reports in 2007 by Kobilka (Stanford Univ.), Stevens (Scripps Research Inst.), Schertler and Tate (Medical Research Council Laboratory of Molecular Biology in Cambridge, UK) and colleagues of the first non-rhodopsin GPCR structure, e.g. the inactive human β_2 adrenergic receptor in complex with the inverse agonist carazolol (Cherezov et al., 2007; Rasmussen et al., 2007; Rosenbaum et al., 2007). These landmark studies were followed by the determination of other GPCRs (**Table 1**), and the rapid pace of these reports is continuing. Biogenic amine receptor complexes (epinephrine, dopamine, histamine, muscarinic), nucleoside (adenosine) receptor complexes, sphingolipid ($S1P_1$) and peptide (CXCR4, opioid) receptor complexes have been reported. All of the crystallized receptors belong to the GPCR family known with the names of Class A, Family 1, or Rhodopsin Family, which in humans comprises over 80% of all GPCRs (Costanzi, 2012; Krishnan et al., 2012). As shown in **Figure 1**, most of these receptors belong to a branch of Class A that comprises receptors for biogenic amines and MECA (melanocortin, endothelial differentiation sphingolipids, cannabinoid and adenosine) receptors. The only exceptions are the chemokine CXCR4 and opioid receptors (κ and μ), which are found in a branch of Class A predominantly populated by peptide receptors, and rhodopsin, which is found in a small branch of Class A populated by opsins. Moreover, the solution of the nociceptin/orphanin FQ peptide receptor has recently been announced. A large portion of the dendrogram of Class A GPCRs, including a branch that comprises mostly receptors for nucleotides and lipids, is still unexplored. There is reason to expect that many other structures will be solved in the near future to shed light onto a still uncharted region of the GPCR phylogenetic dendrogram. Furthermore, the solution of receptors belonging to families beyond Class A is expected.

The technical advances that led to this dramatic progress include: 1) Fusion of the receptor with the T4-lysozyme, which increases the tendency to form crystals – the T4-lysozyme is usually inserted in lieu of the intracellular loop 3 (IL3) (Cherezov et al., 2007; Rosenbaum et al., 2007), but has also been fused with the N-terminus, to facilitate the co-crystallization of a

receptor-G protein complex (Rasmussen et al., 2011b); 2) Structurally-stabilizing point mutations, either in the ligand-binding regions or more remotely – this approach has been introduced by the groups of Schertler and Tate in Cambridge and the associated company Heptares (Warne et al., 2008). These thermostabilizing mutations can be made to favor either an antagonist-bound conformation or agonist-bound conformation (although poorly activatable due to the energetic stabilization) of the same GPCR. The stabilization is so effective that the GPCR protein can be captured on a Biacore chip to allow characterization of small molecule binding by measuring surface plasmon resonance (SPR) (Zhukov et al., 2011); 3) Stabilization of the receptors through antibodies (Rasmussen et al., 2007) – recently, nanobodies generated in llamas inoculated with receptors as well as receptors cross-linked with G protein heterotrimers have been used to solve crystal structures of the activates state of the β_2 adrenergic receptor (Rasmussen et al., 2011a; Rasmussen et al., 2011b) ; 4) Specialized agonists, such as irreversibly binding agonists (Rosenbaum et al., 2011) or an agonist that has multiple arms extending from the core pharmacophore structure (Xu et al., 2011). 5) Specialized techniques for producing crystals of membrane-bound proteins, including adaptation of the lipidic cubic phase, which forms a single lipid-aqueous bilayer that allows ordered protein molecules to make contacts in their hydrophobic as well as hydrophilic portions (Cherezov, 2011).

The ligand binding cavity

All GPCRs are constituted by a single polypeptide chain that spans the plasma membrane seven times with seven alpha helical structures (Costanzi et al., 2009). As the crystal structures revealed, the helical bundle of most Class A GPCRs hosts a ligand binding cavity opened toward the extracellular milieu, which provides access to diffusible ligands. Alternately, the cavities of rhodopsin and $S1P_1$ receptor are sealed from the extracellular space by the second extracellular loop (EL2) and the N-terminus, respectively. It is likely that the hydrophobic ligands of these receptors make their way into the binding cavity through the transmembrane domains. For most GPCRs this ligand binding cavity is lined by transmembrane domains (TMs) 2, 3, 5, 6, and 7 and is deeper in proximity to TMs 5 and 6 while shallower in proximity to TMs 2, and 7 (Figure 2). Nevertheless, in some cases TMs 1 and 4 also form the pocket and can impact ligand binding. The various ligands co-crystallized with their receptors in the currently solved GPCR structures variously occupy different regions of this cavity. This is evident from Figure 3, which shows a

side by side comparison of six representative receptors featuring the bound ligands and the

residues that surround them, as well as Figure 4, which provides an overlay of the same ligands

of these receptors resulting from a structural superposition of the receptors. Notably, different

ligands that bind to the same receptor may occupy different regions of the binding cavity. This

situation is particularly evident from Figure 5A, which compares the binding to the CXCR4

receptor of a small molecule antagonist and a cyclic peptide antagonist (Wu et al., 2010b): there

is virtually no overlap between the two molecules. Less extreme is the case illustrated in Figure

5B, which compares the binding to the adenosine receptor of a non-purine antagonist and an

adenosine-based agonist UK-432097 bearing large substituents at the C2 and N^6 positions of the

purine ring (Xu et al., 2011): although there is substantial overlap between the two molecules,

the larger agonist occupies regions of the receptor unexploited by the antagonist. The ribose

moiety, which is an essential component of nearly all adenosine receptor agonists, confers to the

ligand its agonistic properties. This moiety is accommodated in a space of the binding cavity

close to TM3 that in the antagonist-bound state is unoccupied by a ligand and is partially filled

by water molecules. The hydroxyl and other H-bonding groups of agonists displace these water

molecules, thereby gaining an entropic advantage in the binding process. This is consistent with

the typically nanomolar affinities of agonists at 3 of the 4 subtypes of adenosine receptors. The

other large substituents present on the agonist UK-432097 co-crystallized with the A_{2A} receptor

further enhance the binding affinity of the agonist by establishing contacts with the receptor.

The outer regions of a GPCR can serve as meta-binding sites for a ligand on its path to

the principle orthosteric binding site and can also contribute to the lining of the orthosteric

binding site. In particular, the X-ray structures have confirmed the hypothesis, based on

mutagenesis as well as molecular modeling (Moro et al., 1999; Olah et al., 1994; Peeters et al.,

2011), that parts of the ELs are intimately involved in recognition of ligands for both agonists

and antagonists. Particularly, we now know that the C-terminal part of EL2 tends to drop more or

less deeply, depending on the receptor, into the ligand-binding region to establish contacts with

the ligands (Figure 3), as predicted using site-directed mutagenesis. Peculiar are the cases of

rhodopsin and the $S1P_1$ receptor, in which the ligand-binding cavity is substantially more

enclosed than in other receptors, thanks to a singular conformation of EL2 that occludes the

entrance of the cleft (Palczewski et al., 2000). Conversely, the conformation that EL2 assumes in

the chemokine CXCR4 receptor renders the binding cavity particularly open to the extracellular

space, facilitating the binding of large peptides (Wu et al., 2010b). However, the role of ELs in recognition of and activation by large peptide ligands will require further studies (Dong et al., 2011).

In general, the extracellular loops are typically more varied between subtypes than the TMs, which could facilitate the rational design of more selective orthosteric and allosteric ligands, as guided by the 3D structures of the receptor complexes. For instance, the M_2 (Haga et al., 2012) and M_3 (Kruse et al., 2012) muscarinic acetylcholine receptors contain a vestibule in their outer portions, which corresponds to the regions of the receptor associated with the binding of allosteric modulators. The fact that the orthosteric site of the muscarinic receptors and the specific residues involved in ligand recognition are identical across the family has impeded the medicinal chemical effort to design selective competitive ligands. The possibility of targeting the vestibule, which is more divergent in sequence, offers now further opportunities for drug design. However, for those receptors for which a crystallographically solved structure is not yet available, the high variability of the extracellular regions makes their modeling subject to greater uncertainty when compared to the modeling of the 7 TMs (Goldfeld et al., 2011).

Inactive and activated structures

The determination of both agonist- and antagonist-bound states of the same receptor was accomplished for two classes, i.e. β adrenergic and adenosine receptors, in addition to visual pigment receptors with the structures of opsin and rhodopsin (Choe et al., 2011; Park et al., 2008; Rasmussen et al., 2011a; Rasmussen et al., 2011b; Scheerer et al., 2008; Standfuss et al., 2011; Xu et al., 2011). This major step forward allowed a deeper understanding of the activation processes operating in GPCRs. Thus, the details of agonist binding and activation, i.e. characteristic agonist-induced movement of helices and key residues, are beginning to be understood. The comparison of the structures of inactive rhodopsin with those of the meta II state of rhodopsin as well as the unliganded opsin revealed several conformational changes associated with the activation of the receptor. The most notable of these conformational changes entail outward movements of the intracellular side of TM6 and movements of TM5 toward TM6 (Figures 6A and B). These conformational changes were also found in the agonist-bound $β_2$ adrenergic and A_{2A} adenosine receptors, although the displacement of TM6 is substantially less pronounced in the A_{2A} receptor as a consequence of the T4-lysozyme fused between the

cytosolic ends of TM5 and TM6 (Figure 6C and D). Also, the distance between oppositely charged amino acid side chains near the cytosolic side, e.g. an Arg and an Asp residue respectively found in TMs 3 and 6 and predicted to be involved in a putative ionic lock characteristic of the inactive state, increased upon binding of the agonist in each case. However, it should be noted that this ionic lock was not fully closed in the inactive states of the β_2 adrenergic and A_{2A} adenosine receptors. Furthermore, some movements that were not predicted in the opsin structure were seen in other receptors, such as a see-saw movement of TM7 in the A_{2A} adenosine receptor by which the intracellular end moves inward (Figure 5C and D). Movements in the extracellular loop (EL) regions were also noted. These movements appear to be more ligand-specific than the movements in the TM regions. For example, the outward displacement of EL3 of the A_{2A} adenosine receptor was considerably greater for an agonist having bulky substitutions of the adenine ring than in the unsubstituted cases. Notably, increasing evidence demonstrated that the stimulation of one GPCR can trigger different signaling cascades in a ligand-dependent manner, through a phenomenon known as biased agonism (Kahsai et al., 2011). As a result, the same receptor can be selectively induced to activate a variety of pathways mediated by G proteins as well as β-arrestins. Most likely, these different signaling states are due to distinct conformations of the same receptor that individual ligands can induce or stabilize. Further light will be shed on the correlation between conformation and signaling state of GPCRs once multiple structures of the same receptor with a variety of biased ligands are solved. In this respect some progress has been made for the β_1 and β_2 adrenergic receptors through crystallographic (Warne et al., 2012) and NMR studies (Liu et al., 2012), respectively. For the β_1 adrenergic receptor, the crystal structures revealed that the biased agonists bicindolol and carvedilol, which stimulate β-arrestin-mediated signaling but act as inverse agonists or partial agonists of G protein-dependent pathways, interact with additional residues located in EL2 as well as TM7 when compared to unbiased β blockers. Moreover, the abovementioned NMR spectroscopic analyses of the β_2 adrenergic receptor suggest that ligands, including biased ligands, do not "induce" states but shift equilibrium between preexisting states. Specifically, the study indicates that unbiased ligands impact mostly the conformational state of TM6, while biased agonists shift primarily the conformational state of TM7 (Liu et al., 2012).

Molecular docking at GPCR homology models to predict the structure of receptor ligand complexes

Until recently, the three-dimensional study of the interactions of GPCRs with their ligands was limited to molecular modeling. The modeling efforts began more than two decades ago, using as a crude template the structure of bacteriorhodopsin and progressed with the major advance of the high resolution structure of bovine rhodopsin more than a decade ago (Ballesteros et al., 2001; Costanzi et al., 2007; Costanzi et al., 2009). Although there has been much variability in the confidence in the modeling results (papers were published with diametrically opposed modes of ligand binding for the same receptor ligand-complex), there were examples of well-supported modeling that was later validated crystallographically (among others, see: Ivanov et al., 2009; Michino et al., 2009; Kufareva, 2011). Comparisons of crystal structures and homology models revealed that, for some GPCRs, reasonably accurate receptor-ligand complexes can be constructed through homology modeling followed by molecular docking (Costanzi, 2008; Costanzi, 2010; Costanzi, 2012; Reynolds et al., 2009). However, accurate complexes cannot always be obtained through the sole use of specialized software. Purely computational docking of ligands at GPCR homology models could lead to substantially inaccurate results if the contributions of specific residues to ligand biding or, even worse, the location of the binding cavity are incorrectly recognized. A community wide challenge to molecular modelers to predict the docking mode of antagonist ZM241385 to the A_{2A} adenosine receptor prior to the release of the X-ray structure showed how the ligand could assume almost a random placement around the receptor (Michino et al., 2009). However, when informed with accessory information about the molecular recognition elements, the placement of the ligand in various docking models was shown to be within a reasonable range of accuracy (Michino et al., 2009). In many cases, the identification of the correct receptor-ligand interactions is strictly dependent on an expert selection of the docking poses based on insights derived from site-directed mutagenesis, comparisons of SAR within the same chemical series, and bioinformatics studies within a receptor family.

A further controlled assessment clarified that, when the target receptor shares a significant sequence similarity with one of the available templates, the models are particularly accurate. Conversely, predictions are more challenging for receptors that are more distant from the available templates, in which case the modeling strategies need to be more closely guided

through the incorporation of the abovementioned external information (Kufareva et al., 2011). Since, as we pointed out, there are not yet X-ray structures representative of all major branches of the GPCR dendrogram (**Figure 1**), the modeling of receptors that are more distant from the available templates is still challenging. Moreover, the modeling of GPCRs belonging to classes B and C (Hu et al., 2006; Wheatley et al., 2012) remains more uncertain, since none of the structures of the members of these families have been solved crystallographically.

As mentioned, particularly important is the use of data gathered from site-directed mutagenesis. In this regards, one variation of the use of site-directed mutagenesis that has been particularly informative with respect to probing molecular recognition among GPCRs has been that of reengineering the binding site to accept agonists that have been chemically modified. These approaches, with some important differences, are known by various terms introduced by different reseach groups: RASSLs, neoceptors, and DREADDs (Conklin et al., 2008). Different degrees of design insight vs. empirical screening have been used to match a given mutant receptor with an orthogonally activating agonist analogue. The neoceptor approach, in particular, has focused on the adenosine receptor family to accurately predict the placement of the ribose moiety of nucleoside agonists, using the three-way integrated combination of mutagenesis, modeling, and chemical modification. Complementary changes in the structures of the ligand and receptor that lead to enhanced affinity can help establish the orientation of a ligand within the binding site.

Receptor-ligand interactions can also be studied through a systematic approach that was recently introduced, termed Biophysical Mapping (BPM) (Zhukov et al., 2011). This method is based on the characterization of the functional contour of the binding pocket of a given GPCR using a thermostabilized form of the receptor (StaR). The effects of site-directed mutagenesis within the binding site are correlated with binding data for diverse ligands obtained through SPR measurements. Then, molecular modeling and docking, is used to map the small molecule binding site with respect to each chemical class of ligands. This approach was used to identify novel chemotypes (later to be optimized by chemical modification), such as chromones and triazines, binding to the A_{2A} adenosine receptor (Congreve et al., 2012; Langmead et al., 2012).

Structure-based discovery of GPCR ligands is increasingly more practical

Looking ahead, it will be increasingly feasible to tap the potential of structure-based design for GPCRs, initially for class A (Congreve et al., 2011; Salon et al., 2011) and then, hopefully, for the other classes as well. For now, the newly revealed detailed knowledge of GPCR structures has already facilitated a recent flurry of studies directed toward ligand discovery.

The careful stepwise modification of known classes of agonist or antagonist for a given receptor has been for years a major successful approach of medicinal chemists when applied empirically. This study can now be expedited using accurate 3D knowledge of receptor-ligand recognition. For instance, it is now feasible to target specific amino acid residues in the vicinity of the bound pharmacophore that might confer enhanced affinity or receptor subtype selectivity to the modified ligands. For example, recent reports have shown that A_{2A} adenosine receptor agonists and antagonists can be modified in this manner (Congreve et al., 2012; Deflorian et al., 2012). Moreover, the interaction of small fragments with regions of the binding cavity proximal to the ligand, to be considered as candidate substituents to enhance the receptor-ligand interactions, can also be studied. In this context, in recent study the structure of a known GPCR agonist was systematically varied using the ICM software (Internal Coordinate Mechanics, Molsoft LLC). A library of 2000 small fragments was screened in silico for fit within a small pocket, to successfully predict those favoring adenosine receptor affinity when linked to the 5'-carbonyl group of modified adenosine (Tosh et al., 2012).

For the identification of ligands based on novel chemotypes, a technique that has proven its value is the virtual screening through molecular docking of chemically diverse libraries for the discovery of novel chemotypes that bind to various GPCRs (Costanzi, 2011). A number of controlled experiments targeting the β adrenergic and adenosine receptors, conducted by subjecting to molecular docking known agonists and blockers together with a larger number of non-binders, clearly illustrated that such virtual screening campaigns are most effective when applied to X-ray structures (Costanzi and Vilar, 2012; Reynolds et al., 2009; Vilar et al., 2011a; Vilar et al., 2010). This observation is consistent with the successful identification of novel structurally diverse ligands on the basis of virtual screenings conducted by targeting the crystal structures of β-adrenergic, adenosine, dopamine, and histamine receptors (Carlsson et al., 2011; Carlsson et al., 2010; de Graaf et al., 2011; Katritch et al., 2010a; Kolb et al., 2009; Langmead et al., 2012; Sabio et al., 2008; van der Horst et al., 2011). The abovementioned controlled

experiments also demonstrated that virtual screening campaigns, although not as effective as when applied to a crystal structure, are also useful when applied to accurate homology models (Cavasotto, 2011; Cavasotto et al., 2008; Katritch et al., 2010b; Phatak et al., 2010; Vilar et al., 2011a; Vilar et al., 2010). This observation is in line with the results of virtual screening campaigns through which, prior to the explosion of GPCR crystallography, novel GPCR ligands were identified using rhodopsin-based homology models (Engel et al., 2008; Tikhonova et al., 2008). More recently, Shoichet and coworkers conducted a virtual screening campaign by targeting the crystal structure of the dopamine D_3 receptor as well as a model of the same receptor based on the β_2 adrenergic homologue, with which it shares a relatively high sequence identity (38% within the TMs and 61% within the binding cavity, defined as the residues found within a 4 Å radius from the bound ligands) (Carlsson et al., 2011). Notably, each of these two parallel campaigns yielded two overlapping sets of novel ligands suggesting that models based on a relatively close template are indeed useful to ligand discovery.

Controlled experiments demonstrated also that not only blockers but agonists too are substantially prioritized over non-binders in docking experiments (Costanzi and Vilar, 2012). In particular, such controlled virtual screening campaigns revealed that the activated structure of the β_2 adrenergic receptor is significantly biased toward the preferential recognition of agonists over blockers. Moreover, they also showed that structures of receptors crystallized in the inactive state can be modified in silico by modeling the shape of the binding cavity around a docked agonist, thus being turned into structures that preferentially recognize agonists rather than blockers (Costanzi and Vilar, 2012; Vilar et al., 2011b). However, the identification of agonists based on novel chemotypes through the screening of diverse libraries may prove particularly challenging, in light of the likely stricter structural requirements for agonism than for blockade. Moreover, as mentioned, it is increasingly evident that the same GPCR may trigger a variety of different signaling cascades (Kahsai et al., 2011). The basis for distinguishing ligands needed for selective effector pathway activation (i.e. biased ligands) is an important area for future investigation. Several examples of ligand-specific interactions of the same receptor have been reported, but the implications of these differences for signaling are still largely unknown.

Undoubtedly, docking-based virtual screening campaigns will become increasingly more feasible with the experimental determination of new GPCR structures. Moreover, they will also benefit from the fast pace at which supercomputing is progressing as well as the continuous

improvement of computational algorithms. In particular, the scoring functions that are currently utilized to estimate the likelihood of binding of large sets of screened compounds represent a compromise between accuracy and rapidity. Large computer clusters as well as specialized purpose-built supercomputers will increasingly allow the development and application of more complex methods for the calculation of free binding energies (Mitchell, 2011). Moreover, an increasingly higher number of alternative receptor conformations, either solved experimentally or generated computationally from a single experimental structure, will be applicable in parallel to the screening campaigns. This practice, known as receptor-ensemble docking, was already demonstrated to significantly improve virtual screening yields by providing a means to account for receptor flexibility (Bottegoni et al., 2011; Costanzi, 2011; Costanzi and Vilar, 2012; Vilar et al., 2011a).

Conclusions

Based on methodological advances in X-ray crystallography, the structural elucidation of GPCRs has begun a revolution in the medicinal chemical approaches applied to the discovery of new GPCR ligands. The binding sites of different receptors partly overlap but differ significantly in ligand orientation, depth and breadth of contact areas in TM regions, and the involvement of the extracellular loops (ELs). Conformational changes associated with activation have been analyzed for several receptors. However, there are still large areas where knowledge is lacking. For example there still is an uncharacterized large portion of the GPCR phylogenetic dendrogram, the interaction of large peptide ligands with their receptors are unclear, and the structural basis for functional selectivity, i.e. the reasons behind which agonists display different spectra of activation properties through the same GPCR, are poorly understood. Molecular modeling, informed by supporting information from site-directed mutagenesis and structure activity relationships, has been validated as a useful tool to extend structural insights to related GPCRs and to analyze docking of other ligands in already crystallized GPCRs. Undoubtedly further exploration of the interactions of GPCRs with their G protein and non G-protein intracellular targets, through medicinal chemistry as well as techniques of structural biology, will be required.

Authorship contributions:

Performed data analysis: Costanzi.

Wrote or contributed to the writing of the manuscript: Jacobson, Costanzi.

References

Ballesteros JA, Shi L and Javitch JA (2001) Structural mimicry in G protein-coupled receptors: implications of the high-resolution structure of rhodopsin for structure-function analysis of rhodopsin-like receptors. *Mol Pharmacol* **60**: 1-19.

Bokoch M, Zou Y, Rasmussen S, Liu C, Nygaard R, Rosenbaum D, Fung J, Choi H, Thian F, Kobilka T, Puglisi J, Weis W, Pardo L, Prosser R, Mueller L and Kobilka B (2010) Ligand-specific regulation of the extracellular surface of a G-protein-coupled receptor. *Nature* **463**: 108-112.

Bottegoni G, Rocchia W, Rueda M, Abagyan R, Cavalli A (2011) Systematic exploitation of multiple receptor conformations for virtual ligand screening. *PLoS One* **6**: e18845

Carlsson J, Coleman RG, Setola V, Irwin JJ, Fan H, Schlessinger A, Sali A, Roth BL and Shoichet BK (2011) Ligand discovery from a dopamine D_3 receptor homology model and crystal structure. *Nat Chem Biol* **7**: 769-778.

Carlsson J, Yoo L, Gao Z, Irwin J, Shoichet B and Jacobson K (2010) Structure-based discovery of A_{2A} adenosine receptor ligands. *J Med Chem* **53**: 3748-3755.

Cavasotto CN (2011) Homology models in docking and high-throughput docking. *Curr Top Med Chem* **11**: 1528-1534.

Cavasotto CN, Orry AJ, Murgolo NJ, Czarniecki MF, Kocsi SA, Hawes BE, O'Neill KA, Hine H, Burton MS, Voigt JH, Abagyan RA, Bayne ML and Monsma FJ (2008) Discovery of novel chemotypes to a G-protein-coupled receptor through ligand-steered homology modeling and structure-based virtual screening. *J Med Chem* **51**: 581-588.

Cherezov V (2011) Lipidic cubic phase technologies for membrane protein structural studies. *Curr Opin Struct Biol* **21**: 559-566.

Cherezov V, Rosenbaum D, Hanson M, Rasmussen S, Thian F, Kobilka T, Choi H, Kuhn P, Weis W, Kobilka B and Stevens R (2007) High-resolution crystal structure of an engineered human β2 adrenergic G protein-coupled receptor. *Science* **318**: 1258-1265.

Chien EY, Liu W, Zhao Q, Katritch V, Han GW, Hanson MA, Shi L, Newman AH, Javitch JA, Cherezov V and Stevens RC (2010) Structure of the human dopamine D_3 receptor in complex with a D2/D3 selective antagonist. *Science* **330**: 1091-1095.

Choe HW, Kim YJ, Park JH, Morizumi T, Pai EF, Krauss N, Hofmann KP, Scheerer P and Ernst OP (2011) Crystal structure of metarhodopsin II. *Nature* **471**: 651-655.

Congreve M, Andrews SP, Dore AS, Hollenstein K, Hurrell E, Langmead CJ, Mason JS, Ng IW, Tehan B, Zhukov A, Weir M and Marshall FH (2012) Discovery of 1,2,4-Triazine Derivatives as Adenosine A_{2A} Antagonists using Structure Based Drug Design. *J Med Chem* **55**: 1898-1903.

Congreve M, Langmead CJ, Mason JS and Marshall FH (2011) Progress in Structure Based Drug Design for G Protein-Coupled Receptors. *J Med Chem* **54**: 4283-4311.

Conklin BR, Hsiao EC, Claeysen S, Dumuis A, Srinivasan S, Forsayeth JR, Guettier JM, Chang WC, Pei Y, McCarthy KD, Nissenson RA, Wess J, Bockaert J and Roth BL (2008) Engineering GPCR signaling pathways with RASSLs. *Nat Methods* **5**: 673-678.

Costanzi S (2008) On the applicability of GPCR homology models to computer-aided drug discovery: a comparison between in silico and crystal structures of the β2 adrenergic receptor. *J Med Chem* **51**: 2907-2914.

Costanzi S (2010) Modelling G protein-coupled receptors: a concrete possibility. *Chim Oggi* **28**: 26-30.

Costanzi S (2011) Chapter 18 Structure-based Virtual Screening for Ligands of G Protein-coupled Receptors, in *G Protein-Coupled Receptors: From Structure to Function* (Giraldo J and Pin J-P eds) pp 359-374, The Royal Society of Chemistry.

Costanzi S (2012) Homology modeling of class a g protein-coupled receptors. *Methods Mol Biol* **857**: 259-279.

Costanzi S, Ivanov A, Tikhonova I and Jacobson K (2007) Structure and function of G protein-coupled receptors studied through using sequence analysis, molecular modeling and receptor engineering: adenosine receptors. *Frontiers in Drug Design and Discovery, Bentham* **3**: 63-69.

Costanzi S, Siegel J, Tikhonova I and Jacobson K (2009) Rhodopsin and the others: a historical perspective on structural studies of G protein-coupled receptors. *Curr Pharm Des* **15**: 3994-4002.

Costanzi S and Vilar S (2012) In Silico screening for agonists and blockers of the β_2 adrenergic receptor: Implications of inactive and activated state structures. *J Comput Chem* **33**: 561-572.

de Graaf C, Kooistra AJ, Vischer HF, Katritch V, Kuijer M, Shiroishi M, Iwata S, Shimamura T, Stevens RC, de Esch IJ and Leurs R (2011) Crystal structure-based virtual screening for fragment-like ligands of the human histamine H_1 receptor. *J Med Chem* **54**: 8195-8206.

Deflorian F, Kumar TS, Phan K, Gao ZG, Xu F, Wu H, Katritch V, Stevens RC and Jacobson KA (2012) Evaluation of Molecular Modeling of Agonist Binding in Light of the Crystallographic Structure of an Agonist-Bound A_{2A} Adenosine Receptor. *J Med Chem* **55**: 538-552.

Dong M, Lam PC, Pinon DI, Hosohata K, Orry A, Sexton PM, Abagyan R and Miller LJ (2011) Molecular basis of secretin docking to its intact receptor using multiple photolabile probes distributed throughout the pharmacophore. *J Biol Chem* **286**: 23888-23899.

Dore AS, Robertson N, Errey JC, Ng I, Hollenstein K, Tehan B, Hurrell E, Bennett K, Congreve M, Magnani F, Tate CG, Weir M and Marshall FH (2011) Structure of the Adenosine A_{2A} Receptor in Complex with ZM241385 and the Xanthines XAC and Caffeine. *Structure* **19**: 1283-1293.

Engel S, Skoumbourdis A, Childress J, Neumann S, Deschamps J, Thomas C, Colson A, Costanzi S and Gershengorn M (2008) A virtual screen for diverse ligands: discovery of selective G protein-coupled receptor antagonists. *J Am Chem Soc* **130**: 5115-5123.

Goldfeld DA, Zhu K, Beuming T and Friesner RA (2011) Successful prediction of the intra- and extracellular loops of four G-protein-coupled receptors. *Proc Natl Acad Sci U S A* **108**: 8275-8280.

Granier S, Manglik A, Kruse AC, Kobilka TS, Thian FS, Weis WI and Kobilka BK (2012) Structure of the δ-opioid receptor bound to naltrindole. *Nature* **485**(7398):400-404.

Haga K, Kruse AC, Asada H, Yurugi-Kobayashi T, Shiroishi M, Zhang C, Weis WI, Okada T, Kobilka BK, Haga T and Kobayashi T (2012) Structure of the human M2 muscarinic acetylcholine receptor bound to an antagonist. *Nature* **482**: 547-551.

Hanson M, Cherezov V, Griffith M, Roth C, Jaakola V, Chien E, Velasquez J, Kuhn P and Stevens R (2008) A specific cholesterol binding site is established by the 2.8 A structure of the human β_2 adrenergic receptor. *Structure* **16**: 897-905.

Hanson MA, Roth CB, Jo E, Griffith MT, Scott FL, Reinhart G, Desale H, Clemons B, Cahalan SM, Schuerer SC, Sanna MG, Han GW, Kuhn P, Rosen H and Stevens RC (2012) Crystal structure of a lipid G protein-coupled receptor. *Science* **335**: 851-855.

Hino T, Arakawa T, Iwanari H, Yurugi-Kobayashi T, Ikeda-Suno C, Nakada-Nakura Y, Kusano-Arai O, Weyand S, Shimamura T, Nomura N, Cameron AD, Kobayashi T, Hamakubo T, Iwata S and Murata T (2012) G-protein-coupled receptor inactivation by an allosteric inverse-agonist antibody. *Nature* **482**: 237-240.

Hu J, Jiang J, Costanzi S, Thomas C, Yang W, Feyen J, Jacobson K and Spiegel A (2006) A missense mutation in the seven-transmembrane domain of the human Ca^{2+} receptor converts a negative allosteric modulator into a positive allosteric modulator. *J Biol Chem* **281**: 21558-21565.

Ivanov A, Barak D and Jacobson K (2009) Evaluation of homology modeling of G-protein-coupled receptors in light of the A_{2A} adenosine receptor crystallographic structure. *J Med Chem* **52**: 3284-3292.

Jaakola V, Griffith M, Hanson M, Cherezov V, Chien E, Lane J, IJzerman A and Stevens R (2008) The 2.6 angstrom crystal structure of a human A_{2A} adenosine receptor bound to an antagonist. *Science* **322**: 1211-1217.

Kahsai AW, Xiao K, Rajagopal S, Ahn S, Shukla AK, Sun J, Oas TG and Lefkowitz RJ (2011) Multiple ligand-specific conformations of the β_2 adrenergic receptor. *Nat Chem Biol* **7**: 692-700.

Katritch V, Jaakola V, Lane J, Lin J, IJzerman A, Yeager M, Kufareva I, Stevens R and Abagyan R (2010a) Structure-based discovery of novel chemotypes for adenosine A_{2A} receptor antagonists. *J Med Chem* **53**: 1799-1809.

Katritch V, Rueda M, Lam P, Yeager M and Abagyan R (2010b) GPCR 3D homology models for ligand screening: lessons learned from blind predictions of adenosine A_{2A} receptor complex. *Proteins* **78**: 197-211.

Kolb P, Rosenbaum D, Irwin J, Fung J, Kobilka B and Shoichet B (2009) Structure-based discovery of β_2 adrenergic receptor ligands. *Proc Natl Acad Sci U S A* **106**: 6843-6848.

Krishnan A, Almen MS, Fredriksson R and Schioth HB (2012) The origin of GPCRs: identification of mammalian like Rhodopsin, Adhesion, Glutamate and Frizzled GPCRs in fungi. *PLoS One* **7**: e29817.

Kruse AC, Hu J, Pan AC, Arlow DH, Rosenbaum DM, Rosemond E, Green HF, Liu T, Chae PS, Dror RO, Shaw DE, Weis WI, Wess J and Kobilka BK (2012) Structure and dynamics of the M3 muscarinic acetylcholine receptor. *Nature* **482**: 552-556.

Kufareva I, Rueda M, Katritch V, Stevens RC and Abagyan R (2011) Status of GPCR modeling and docking as reflected by community-wide GPCR Dock 2010 assessment. *Structure* **19**: 1108-1126.

Langmead CJ, Andrews SP, Congreve M, Errey JC, Hurrell E, Marshall FH, Mason JS, Richardson CM, Robertson N, Zhukov A and Weir M (2012) Identification of Novel Adenosine A_{2A} Receptor Antagonists by Virtual Screening. *J Med Chem* **55**: 1904-1909.

Lebon G, Warne T, Edwards PC, Bennett K, Langmead CJ, Leslie AG and Tate CG (2011) Agonist-bound adenosine A_{2A} receptor structures reveal common features of GPCR activation. *Nature* **474**: 521-555.

Li J, Edwards PC, Burghammer M, Villa C and Schertler GF (2004) Structure of bovine rhodopsin in a trigonal crystal form. *J Mol Biol* **343**: 1409-1438.

Liu JJ, Horst R, Katritch V, Stevens RC and Wüthrich (2012) Biased signaling pathways in β_2-adrenergic receptor characterized by ^{19}F-NMR. *Science* **335**: 1106-1110.

Makino CL, Riley CK, Looney J, Crouch RK and Okada T (2010) Binding of more than one retinoid to visual opsins. *Biophys J* **99**: 2366-2373.

Manglik A, Kruse AC, Kobilka TS, Thian FS, Mathiesen JM, Sunahara RK, Pardo L, Weis WI, Kobilka BK and Granier S (2012) Crystal structure of the mu-opioid receptor bound to a morphinan antagonist. *Nature* **485**: 321-326.

Michino M, Abola E, 2008 Participants G, Brooks Cr, Dixon J, Moult J and Stevens R (2009) Community-wide assessment of GPCR structure modelling and ligand docking: GPCR Dock 2008. *Nat Rev Drug Discov* **8**: 455-463.

Mitchell W, Matsumoto S (2011) Large-scale integrated super-computing platform for next generation virtual drug discovery. *Curr Opin Chem Biol* **15**: 553-559.

Moro S, Hoffmann C and Jacobson KA (1999) Role of the extracellular loops of G protein-coupled receptors in ligand recognition: a molecular modeling study of the human $P2Y_1$ receptor. *Biochemistry* **38**: 3498-3507.

Moukhametzianov R, Warne T, Edwards PC, Serrano-Vega MJ, Leslie AG, Tate CG and Schertler GF (2011) Two distinct conformations of helix 6 observed in antagonist-bound structures of a β_1 adrenergic receptor. *Proc Natl Acad Sci U S A* **108**: 8228-8232.

Murakami M and Kouyama T (2008) Crystal structure of squid rhodopsin. *Nature* **453**: 363-367.

Murakami M and Kouyama T (2011) Crystallographic analysis of the primary photochemical reaction of squid rhodopsin. *J Mol Biol* **413**: 615-627.

Nakamichi H, Buss V and Okada T (2007) Photoisomerization mechanism of rhodopsin and 9-cis-rhodopsin revealed by x-ray crystallography. *Biophys J* **92**: L106-108.

Nakamichi H and Okada T (2006a) Crystallographic analysis of primary visual photochemistry. *Angew Chem Int Ed Engl* **45**: 4270-4273.

Nakamichi H and Okada T (2006b) Local peptide movement in the photoreaction intermediate of rhodopsin. *Proc Natl Acad Sci U S A* **103**: 12729-12734.

Okada T, Fujiyoshi Y, Silow M, Navarro J, Landau EM and Shichida Y (2002) Functional role of internal water molecules in rhodopsin revealed by X-ray crystallography. *Proc Natl Acad Sci U S A* **99**: 5982-5987.

Okada T, Sugihara M, Bondar AN, Elstner M, Entel P and Buss V (2004) The retinal conformation and its environment in rhodopsin in light of a new 2.2 A crystal structure. *J Mol Biol* **342**: 571-583.

Olah M, Jacobson K and Stiles G (1994) Role of the second extracellular loop of adenosine receptors in agonist and antagonist binding. Analysis of chimeric A_1/A_3 adenosine receptors. *J Biol Chem* **269**: 24692-24698.

Palczewski K, Kumasaka T, Hori T, Behnke CA, Motoshima H, Fox BA, Le Trong I, Teller DC, Okada T, Stenkamp RE, Yamamoto M and Miyano M (2000) Crystal structure of rhodopsin: A G protein-coupled receptor. *Science* **289**: 739-745.

Park JH, Scheerer P, Hofmann KP, Choe HW and Ernst OP (2008) Crystal structure of the ligand-free G-protein-coupled receptor opsin. *Nature* **454**: 183-187.

Peeters MC, van Westen GJ, Li Q and IJzerman AP (2011) Importance of the extracellular loops in G protein-coupled receptors for ligand recognition and receptor activation. *Trends Pharmacol Sci* **32**: 35-42.

Phatak SS, Gatica EA and Cavasotto CN (2010) Ligand-Steered Modeling and Docking: A Benchmarking Study in Class A G-Protein-Coupled Receptors. *J Chem Inf Model* **50**: 2119-2128.

Rasmussen S, Choi H, Rosenbaum D, Kobilka T, Thian F, Edwards P, Burghammer M, Ratnala V, Sanishvili R, Fischetti R, Schertler G, Weis W and Kobilka B (2007) Crystal structure of the human β_2 adrenergic G-protein-coupled receptor. *Nature* **450**: 383-387.

Rasmussen SG, Choi HJ, Fung JJ, Pardon E, Casarosa P, Chae PS, Devree BT, Rosenbaum DM, Thian FS, Kobilka TS, Schnapp A, Konetzki I, Sunahara RK, Gellman SH, Pautsch A, Steyaert J, Weis WI and Kobilka BK (2011a) Structure of a nanobody-stabilized active state of the β_2 adrenoceptor. *Nature* **469**: 175-180.

Rasmussen SG, DeVree BT, Zou Y, Kruse AC, Chung KY, Kobilka TS, Thian FS, Chae PS, Pardon E, Calinski D, Mathiesen JM, Shah ST, Lyons JA, Caffrey M, Gellman SH, Steyaert J, Skiniotis G, Weis WI, Sunahara RK and Kobilka BK (2011b) Crystal structure of the β_2 adrenergic receptor-Gs protein complex. *Nature* **477**: 549-555.

Reynolds K, Katritch V and Abagyan R (2009) Identifying conformational changes of the β_2 adrenoceptor that enable accurate prediction of ligand/receptor interactions and screening for GPCR modulators. *J Comput Aided Mol Des* **23**: 273-288.

Rosenbaum D, Cherezov V, Hanson M, Rasmussen S, Thian F, Kobilka T, Choi H, Yao X, Weis W, Stevens R and Kobilka B (2007) GPCR engineering yields high-resolution structural insights into β_2 adrenergic receptor function. *Science* **318**: 1266-1273.

Rosenbaum DM, Zhang C, Lyons JA, Holl R, Aragao D, Arlow DH, Rasmussen SG, Choi HJ, Devree BT, Sunahara RK, Chae PS, Gellman SH, Dror RO, Shaw DE, Weis WI, Caffrey M, Gmeiner P and Kobilka BK (2011) Structure and function of an irreversible agonist-β_2 adrenoceptor complex. *Nature* **469**: 236-240.

Sabio M, Jones K and Topiol S (2008) Use of the X-ray structure of the β_2 adrenergic receptor for drug discovery. Part 2: Identification of active compounds. *Bioorg Med Chem Lett* **18**: 5391-5395.

Salom D, Lodowski D, Stenkamp R, Le Trong I, Golczak M, Jastrzebska B, Harris T, Ballesteros J and Palczewski K (2006) Crystal structure of a photoactivated deprotonated intermediate of rhodopsin. *Proc Natl Acad Sci U S A* **103**: 16123-16128.

Salon JA, Lodowski DT and Palczewski K (2011) The significance of G protein-coupled receptor crystallography for drug discovery. *Pharmacol Rev* **63**: 901-937.

Scheerer P, Park JH, Hildebrand PW, Kim YJ, Krauss N, Choe HW, Hofmann KP and Ernst OP (2008) Crystal structure of opsin in its G-protein-interacting conformation. *Nature* **455**: 497-502.

Shimamura T, Hiraki K, Takahashi N, Hori T, Ago H, Masuda K, Takio K, Ishiguro M and Miyano M (2008) Crystal structure of squid rhodopsin with intracellularly extended cytoplasmic region. *J Biol Chem* **283**: 17753-17756.

Shimamura T, Shiroishi M, Weyand S, Tsujimoto H, Winter G, Katritch V, Abagyan R, Cherezov V, Liu W, Han GW, Kobayashi T, Stevens RC and Iwata S (2011) Structure of the human histamine H_1 receptor complex with doxepin. *Nature* **475**: 65-70.

Standfuss J, Edwards PC, D'Antona A, Fransen M, Xie G, Oprian DD and Schertler GF (2011) The structural basis of agonist-induced activation in constitutively active rhodopsin. *Nature* **471**: 656-660.

Standfuss J, Xie G, Edwards PC, Burghammer M, Oprian DD and Schertler GF (2007) Crystal structure of a thermally stable rhodopsin mutant. *J Mol Biol* **372**: 1179-1188.

Stenkamp RE (2008) Alternative models for two crystal structures of bovine rhodopsin. *Acta Crystallogr D Biol Crystallogr* **D64**: 902-904.

Teller DC, Okada T, Behnke CA, Palczewski K and Stenkamp RE (2001) Advances in determination of a high-resolution three-dimensional structure of rhodopsin, a model of G-protein-coupled receptors (GPCRs). *Biochemistry* **40**: 7761-7772.

Tikhonova I, Sum C, Neumann S, Engel S, Raaka B, Costanzi S and Gershengorn M (2008) Discovery of novel agonists and antagonists of the free fatty acid receptor 1 (FFAR1) using virtual screening. *J Med Chem* **51**: 625-633.

Thompson AA, Liu W, Chun E, Katritch V, Wu H, Vardy E, Huang X-P, Trapella C, Guerrini R, Calo G, Roth BL, Cherezov V and Stevens RC (2012) Structure of the nociceptin/orphanin FQ receptor in complex with a peptide mimetic. *Nature* **485**: 395-399.

Tosh DK, Phan K, Gao ZG, Gakh A, Xu F, Deflorian F, Abagyan R, Stevens RC, Jacobson KA and Katritch V (2012) Optimization of adenosine 5'-carboxamide derivatives as adenosine receptor agonists using structure-based ligand design and fragment-based searching. *J Med Chem* **55**: 4297-4308.

van der Horst E, van der Pijl R, Mulder-Krieger T, Bender A and IJzerman AP (2011) Substructure-based virtual screening for adenosine A_{2A} receptor ligands. *ChemMedChem* **6**: 2302-2311.

Vilar S, Ferino G, Phatak SS, Berk B, Cavasotto CN and Costanzi S (2011a) Docking-based virtual screening for ligands of G protein-coupled receptors: not only crystal structures but also in silico models. *J Mol Graph Model* **29**: 614-623.

Vilar S, Karpiak J, Berk B and Costanzi S (2011b) In silico analysis of the binding of agonists and blockers to the β_2 adrenergic receptor. *J Mol Graph Model* **29**: 809-817.

Vilar S, Karpiak J and Costanzi S (2010) Ligand and structure-based models for the prediction of ligand-receptor affinities and virtual screenings: Development and application to the β_2 adrenergic receptor. *J Comput Chem* **31**: 707-720.

Wacker D, Fenalti G, Brown MA, Katritch V, Abagyan R, Cherezov V and Stevens RC (2010) Conserved binding mode of human β_2 adrenergic receptor inverse agonists and antagonist revealed by X-ray crystallography. *J Am Chem Soc* **132**: 11443-11445.

Warne T, Edwards PC, Leslie AG and Tate CG (2012) Crystal structures of a stabilized β_1 adrenoceptor bound to the biased agonists bucindolol and carvedilol. *Structure* **20**: 841-849.

Warne T, Moukhametzianov R, Baker JG, Nehme R, Edwards PC, Leslie AG, Schertler GF and Tate CG (2011) The structural basis for agonist and partial agonist action on a β_1 adrenergic receptor. *Nature* **469**: 241-244.

Warne T, Serrano-Vega M, Baker J, Moukhametzianov R, Edwards P, Henderson R, Leslie A, Tate C and Schertler G (2008) Structure of a β_1 adrenergic G-protein-coupled receptor. *Nature* **454**: 486-491.

Wheatley M, Wootten D, Conner MT, Simms J, Kendrick R, Logan RT, Poyner DR and Barwell J (2012) Lifting the lid on GPCRs: the role of extracellular loops. *Br J Pharmacol* **165**: 1688-1703.

Wu B, Chien EY, Mol CD, Fenalti G, Liu W, Katritch V, Abagyan R, Brooun A, Wells P, Bi FC, Hamel DJ, Kuhn P, Handel TM, Cherezov V and Stevens RC (2010) Structures of the CXCR4 chemokine GPCR with small-molecule and cyclic peptide antagonists. *Science* **330**: 1066-1071.

Wu H, Wacker D, Mileni M, Katritch V, Han GW, Vardy E, Liu W, Thompson AA, Huang XP, Carroll FI, Mascarella SW, Westkaemper RB, Mosier PD, Roth BL, Cherezov V and Stevens RC (2012) Structure of the human kappa-opioid receptor in complex with JDTic. *Nature* **485**: 327-332.

Xu F, Wu H, Katritch V, Han GW, Jacobson KA, Gao ZG, Cherezov V and Stevens RC (2011)
    Structure of an Agonist-Bound Human A$_{2A}$ Adenosine Receptor. *Science* **332**: 322-327.
Zhukov A, Andrews SP, Errey JC, Robertson N, Tehan B, Mason JS, Marshall FH, Weir M and
    Congreve M (2011) Biophysical mapping of the adenosine A$_{2A}$ receptor. *J Med Chem* **54**:
    4312-4323.

Footnote:

This work was supported by the National Institutes of Health, National Institute of Diabetes and Digestive and Kidney Diseases [Grant Z01 DK031126-08].

Figure legends

Figure 1. Phylogenetic dendrogram of family A GPCRs based on aligned sequences. All the family members with solved crystal structures, with the exception of rhodopsin, the CXCR4 chemokine receptor, and the δ, κ and μ opioid receptors and the nociceptin/orphanin FQ (NOP) receptor, belong to a cluster of receptors for biogenic amines and MECA (melanocortin, endothelial differentiation sphingolipids, cannabinoid and adenosine) receptors.

Figure 2. Side-by-side comparison of the crystal structures of six representative receptors. All receptors show a common topology composed of seven transmembrane α helices connected by three extracellular and three intracellular loops. The N-terminus is in the extracellular space while the C-terminus is in the cytosol. The co-crystallized ligands and are found within an interhelical cavity open toward the extracellular milieu. The backbone of the receptors is schematically represented as a cartoon, with a color gradient ranging from blue at the N-terminus to red at the C-terminus (TM1: dark blue, TM2: pale blue; TM3: blue/green; TM4 green; TM5: yellow; TM6: yellow/orange; TM7: orange/red). The co-crystallized ligands are represented as van der Waals spheres, with the carbon atoms colored in charcoal grey, oxygen atoms in red, nitrogen atoms in blue and sulfur atoms in yellow.

Figure 3. The shown co-crystallized ligands – all antagonists or inverse agonists – are retinal for rhodopsin, carazolol (1-(9H-carbazol-4-yloxy)-3-(propan-2-ylamino)propan-2-ol) for the β_2 adrenergic receptor, ZM241385 (4-(2-(7-amino-2-(furan-2-yl)-[1,2,4]triazolo[1,5-a][1,3,5]triazin-5-ylamino)ethyl)phenol) for the A_{2A} adenosine receptor, tiotropium ((1α,2β,4β,7β)-7-[(hydroxidi-2-thienylacetyl)oxy]-9,9-dimethyl-3-oxa-9-azoniatricyclo[3.3.1.0^{2,4}]nonane bromide) for the muscarinic M_3 receptor, the small molecule antagonist IT1t (6-dimethyl-5H,6H-imidazo[2,1-b][1,3]thiazol-3-yl}methyl)sulfanyl]methanimidamide) for the CXCR4 receptor and ML056 ((R)-3-amino-(3-hexylphenylamino)-4-oxobutylphosphonic acid) for the $S1P_1$ receptor. Color-coded labels indicate the 7 TMs, while, for selected residues, black labels indicate the GPCR residue index. The alignment of the 6 panels derives from a superposition of the receptors, which are

oriented with their axis perpendicular to the plane of the membrane as in **Figure 2**. To facilitate a comparison of the structural alignment of the binding cavities, dashed lines are drawn that intersect in correspondence to the conserved proline residue found in TM6 (P6.50 according to the GPCR residue indexing system). The red lines are parallel to the plane of the membrane, while the blue lines are perpendicular to it. As is evident, some ligands bind more deeply than others. Moreover, some ligands bind more toward TM5 (to the left of the blue line), while others bind more in the direction of TM2 (the right of the blue line).

Figure 4. Panel a shows an overlay of the six ligands of the six representative receptors shown in **Figures 1** and **2**, resulting from a structural superposition of the receptors – retinal in gray, carazolol in green, ZM241385 in pink, tiotropium in dark red, IT1t in blue/purple, ML056 in yellow. For the A_{2A} adenosine receptor the agonist UK-432097 (2-(3-[1-(pyridin-2-yl)piperidin-4-yl]ureido)ethyl-6-N-(2,2-diphenylethyl)-5′-N-ethylcarboxamidoadenosine-2-carboxamide), in magenta, is also shown. In panel b, the same ligands are shown within the backbone of the A_{2A} receptor. For further explanation on the representation of the receptor, see the legend of **Figure 2**.

Figure 5. Comparison of the binding mode of different ligands to the CXCR4 receptor (a) and the A_{2A} adenosine receptor (b). In the case of the CXCR4 receptor, there is virtually no overlap between the bound small molecule antagonist IT1t (pale blue) and the cyclic peptide antagonist CVX15 (cyclic disulfide of H-Arg-Arg-Nal-Cys-Tye-Gln-Lys-D-Pro-Pro-Tyr-Arg-Cit-Cys-Arg-Gly- D-Pro-OH, pale pink). In the case of the adenosine receptor there is more commonality between the binding mode of the two ligands, but the larger agonist (pale blue) touches areas of the receptor that do not interact with the antagonist (pale pink). The ligands are represented as van der Waals spheres. For further explanation on the representation of the receptor, see the legend of **Figure 2**.

Figure 6. Comparison of inactive and activated structures for rhodopsin (panels a and b) and for the A_{2A} adenosine receptor (panels c and d). A seesaw movement of TM7 that is shifted toward the core of the receptor in the agonist bound structure is more evident in the A_{2A} receptor than in rhodopsin (yellow arrows in panels a and c). Conversely, an outward

movement of TM6 (yellow arrows in panels b and d) is more evident in rhodopsin than the adenosine A_{2A} receptor, where the conformational change might have been hindered by the presence of a T4-lysozyme fused between TMs 5 and 6. The cartoon representations of the receptors are colored in green for the activated receptors according to the scheme outlined in the legend of **Figure 2** for the inactive receptors. The ligands are represented as van der Waals spheres, with the agonists colored in pale blue and the blockers colored in pale pink.

Table 1. Crystal structures of GPCRs deposited in the Protein Data Bank (www.rcsb.org) at the time of this writing.

A total of 73 structures for 15 distinct receptors have been published, namely: 20 for bovine rhodopsin, 4 for squid

rhodopsin, 12 for the β_1 adrenergic receptor, 11 for the β_2 adrenergic receptor, 11 for the A_{2A} adenosine receptor, 5

for the CXCR4 chemokine receptor, 1 for the D_3 dopamine receptor, 1 for the H_1 histamine receptor, 1 for the M_2

muscarinic acetylcholine receptor, 1 for the M_3 muscarinic receptor, 2 for the $S1P_1$ receptor, 1 for the κ opioid

receptor, 1 for the μ opioid receptor, 1 for the δ opioid receptor and 1 for the nociceptin/orphanin FQ (NOP)

receptor.

Receptor	PDB ID	Ligand	Putative State	Res. (Å)	Reference
Bovine rhodopsin	1F88	11-cis-retinal	ground state	2.80	(Palczewski et al., 2000)
	1HZX	11-cis-retinal	ground state	2.80	(Teller et al., 2001)
	1L9H	11-cis-retinal	ground state	2.60	(Okada et al., 2002)
	1U19	11-cis-retinal	ground state	2.20	(Okada et al., 2004)
	1GZM	11-cis-retinal	ground state	2.65	(Li et al., 2004)
	2G87	all-trans-retinal (distorted)	bathorhodopsin	2.60	(Nakamichi and Okada, 2006a)
	2HPY	all-trans-retinal	lumirhodopsin	2.80	(Nakamichi and Okada, 2006b)
	2I35	11-cis-retinal	ground state	3.80	(Salom et al., 2006)
	2I36	11-cis-retinal	ground state	4.10	(Salom et al., 2006)
	2I37 [a,b]	all-trans retinal	early photoactivation intermediate	4.15	(Salom et al., 2006)
	2PED	9-cis-retinal	isorhodopsin	3.40	(Nakamichi et al., 2007)
	2J4Y [c]	11-cis-retinal	ground state	2.65	(Standfuss et al., 2007)
	3C9L [d]	11-cis-retinal	ground state	3.40	(Stenkamp, 2008)
	3C9M [e]	11-cis-retinal	ground state	2.60	(Stenkamp, 2008)
	3CAP [b]	unliganded	activated opsin	2.90	(Park et al., 2008)
	3DQB [f]	unliganded	activated opsin	2.70	(Scheerer et al., 2008)
	3OAX	11-cis-retinal and β-ionone	ground state	2.95	(Makino et al., 2010)
	2X72 [f,g]	all-trans retinal	metarhodopsin II	3.00	(Standfuss et al., 2011)
	3PQR [f]	all-trans retinal	metarhodopsin II	2.85	(Choe et al., 2011)
	3PXO	all-trans retinal	metarhodopsin II	3.00	(Choe et al., 2011)
Squid rhodopsin	2ZIY	11-cis-retinal	ground state	3.70	(Shimamura et al., 2008)
	2Z73	11-cis-retinal	ground state	2.50	(Murakami and Kouyama, 2008)
	3AYM	all-trans-retinal	bathorhodopsin	2.80	(Murakami and Kouyama, 2011)
	3AYN	9-cis-retinal	isorhodopsin	2.70	(Murakami and Kouyama, 2011)
Turkey β_1 adrenergic receptor	2VT4 [c]	cyanopindolol (antagonist)	inactive	2.70	(Warne et al., 2008)
	2Y00 [c]	dobutamine (partial agonist)	inactive	2.50	(Warne et al., 2011)
	2Y01 [c]	dobutamine (partial agonist)	inactive	2.60	(Warne et al., 2011)
	2Y02 [c]	carmoterol (full agonist)	inactive	2.60	(Warne et al., 2011)
	2Y03 [c]	isoprenaline (full agonist)	inactive	2.85	(Warne et al., 2011)
	2Y04 [c]	salbutamol (partial agonist)	inactive	3.05	(Warne et al., 2011)
	2YCW [c,h]	carazolol (antagonist)	inactive	3.00	(Moukhametzianov et al., 2011)
	2YCX [c,h]	cyanopindolol (antagonist)	inactive	3.25	(Moukhametzianov et al., 2011)

	2YCY [c]	cyanopindolol (antagonist)	inactive	3.15	(Moukhametzianov et al., 2011)
	2YCZ [c]	iodocyanopindolol (antagonist)	inactive	3.65	(Moukhametzianov et al., 2011)
	4AMI [c]	bucindolol (biased agonist)	inactive	3.20	(Warne et al., 2012)
	4AMJ [c]	carvedilol (biased agonist)	inactive	2.30	(Warne et al., 2012)
Human β_2 adrenergic receptor	2R4R [i,a]	carazolol (inverse agonist) [1]	inactive	3.40	(Rasmussen et al., 2007)
	2R4S [i,a]	carazolol (inverse agonist) [1]	inactive	3.40	(Rasmussen et al., 2007)
	2RH1 [j,b]	carazolol (inverse agonist)	inactive	2.40	(Cherezov et al., 2007; Rosenbaum et al., 2007)
	3D4S [j]	timolol (inverse agonist)	inactive	2.80	(Hanson et al., 2008)
	3KJ6 [i,a]	carazolol (inverse agonist)	inactive	3.40	(Bokoch et al., 2010)
	3NY8 [j]	ICI 118551 (inverse agonist)	inactive	2.84	(Wacker et al., 2010)
	3NY9 [j]	recent comp. (inverse-agonist)	inactive	2.84	(Wacker et al., 2010)
	3NYA [j]	alprenolol (antagonist)	inactive	3.16	(Wacker et al., 2010)
	3PDS [j]	FAUC50 (irreversible agonist)	inactive	3.50	(Rosenbaum et al., 2011)
	3P0G [j,k]	BI-167107 (agonist)	activated	3.50	(Rasmussen et al., 2011a)
	3SN6 [j,k,l]	BI-167107 (agonist)	activated	3.20	(Rasmussen et al., 2011b)
Human A_{2A} adenosine receptor	3EML [j]	ZM241385 (antagonist)	inactive	2.60	(Jaakola et al., 2008)
	2YDO [c]	adenosine (agonist)	inactive	3.00	(Lebon et al., 2011)
	2YDV [c]	NECA (agonist)	inactive	2.60	(Lebon et al., 2011)
	3QAK [j]	UK-432097	activated	2.71	(Xu et al., 2011)
	3PWH [c]	ZM241385 (antagonist)	inactive	3.30	(Dore et al., 2011)
	3REY [c]	XAC (antagonist)	inactive	3.31	(Dore et al., 2011)
	3RFM [c]	caffeine (antagonist)	inactive	3.60	(Dore et al., 2011)
	3VG9 [m]	ZM241385 (antagonist)	inactive	2.70	(Hino et al., 2012)
	3VGA [m]	ZM241385 (antagonist)	inactive	3.10	(Hino et al., 2012)
	3UZA [c]	1,2,4-triazine 4e (antagonist)	inactive	3.27	(Congreve et al., 2012)
	3UZC [c]	1,2,4-triazine 4g (antagonist)	inactive	3.24	(Congreve et al., 2012)
Human CXCR4 chemokine receptor	3ODU [j,b]	IT1t (small mol. antagonists)	Inactive	2.50	(Wu et al., 2010)
	3OE9 [j,b]	IT1t (small mol. antagonists)	inactive	3.10	(Wu et al., 2010)
	3OE8 [j,b]	IT1t (small mol. antagonists)	inactive	3.10	(Wu et al., 2010)
	3OE6 [j,b]	IT1t (small mol. antagonists)	inactive	3.20	(Wu et al., 2010)
	3OE0 [j,b]	CVX15 (peptide antagonist)	inactive	2.90	(Wu et al., 2010)
Human D_3 dopamine receptor	3PBL [j]	eticlopride (antagonist)	inactive	2.89	(Chien et al., 2010)
Human H_1 histamine receptor	3RZE [j]	doxepin (antagonist)	inactive	3.10	(Shimamura et al., 2011)
Human M_2 Muscarinic receptor	3UON [j]	3-quinuclidinyl-benzilate (antagonist)	inactive	3.00	(Haga et al., 2012)
Rat M_3 Muscarinic receptor	4DAJ [j]	Tiotropium (inverse agonist)	inactive	3.40	(Kruse et al., 2012)
Human $S1P_1$ sphingosine 1-phosphate receptor	3V2Y [j,n]	ML056 (antagonist)	inactive	2.80	(Hanson et al., 2012)
	3V2W [j]	ML056 (antagonist)	inactive	3.35	(Hanson et al., 2012)
Human κ	4DJH [h,k]	JDTic (antagonist)	inactive	2.90	(Wu et al., 2012)

opioid receptor					
Mouse μ opioid receptor	4DKL [j,b]	β-funaltrexamine (irreversible antagonist)	inactive	2.80	(Manglik et al., 2012)
Mouse δ opioid receptor	4EJ4 [j,b]	Naltrindole (antagonist)	inactive	3.40	(Granier et al., 2012)
Human nociceptin/ orphanin FQ (NOP) receptor	4EA3 [o]	Peptide mimetic c-24 (antagonist)	inactive	3.01	(Thompson et al., 2012)

[a] Ligand not visible.

[b] Potentially biologically relevant dimer observed in the structure

[c] Thermally stable mutant receptor.

[d] Alternative model of 1GZM.

[e] Alternative model of 2J4Y.

[f] In complex with a C-terminal peptide of the α-subunit of transducin.

[g] Constitutively active mutant

[h] Showing an intact salt bridge linking the cytoplasmic ends of TMs 3 and 6

[i] In complex with a Fab.

[j] T4-lysozyme fusion protein.

[k] In complex with a camelid antibody fragment

[l] In complex with a G protein (G_s) heterotrimer

[m] In complex with a Fab that prevents agonist binding.

[n] Processed with a microdiffraction data assembly method.

[o] Fusion protein with thermostabilized apocytochrome b_{562}RIL (BRIL).
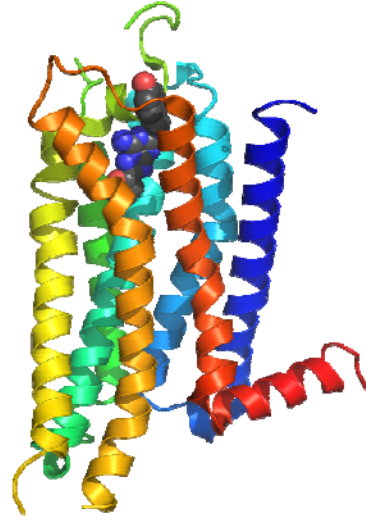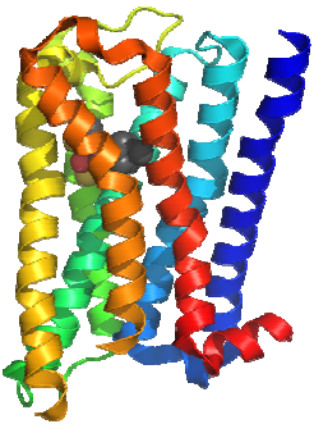
Figure 1
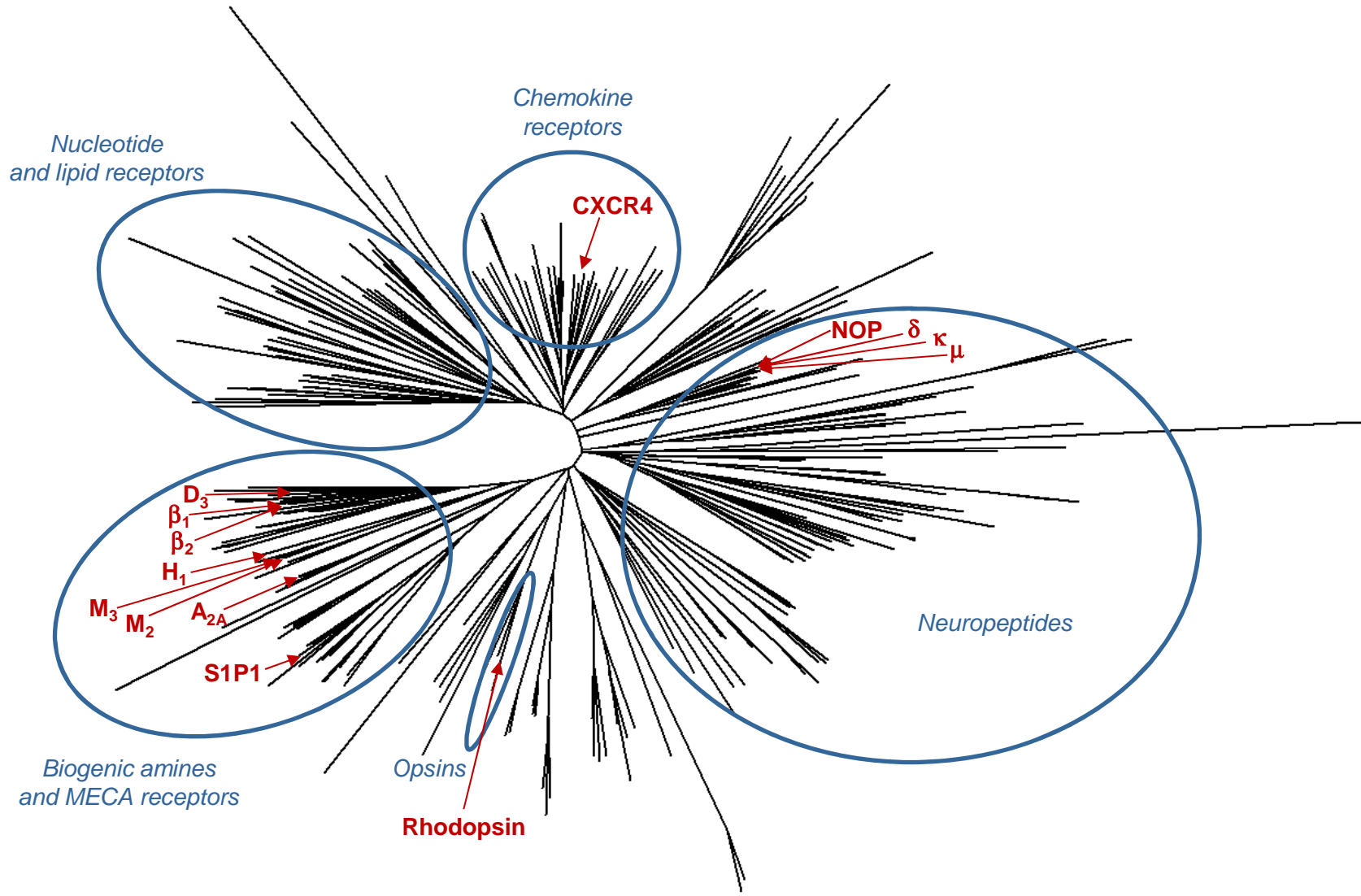
Figure 2

Rhodopsin
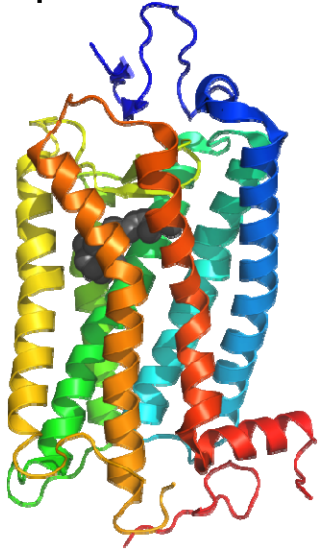
β₂

A₂ₐ

M₃

CXCR4

S1P1

Figure 3

Rhodopsin

EL2

TM3

TM5

TM7

TM6

β₂

EL2

TM3

TM5

TM7

TM6

A₂ₐ

EL3

EL2

TM5

TM7

TM3 hidden by ligand

TM6

M₃

TM5

TM7

TM3

TM6

TM4 hidden by ligand
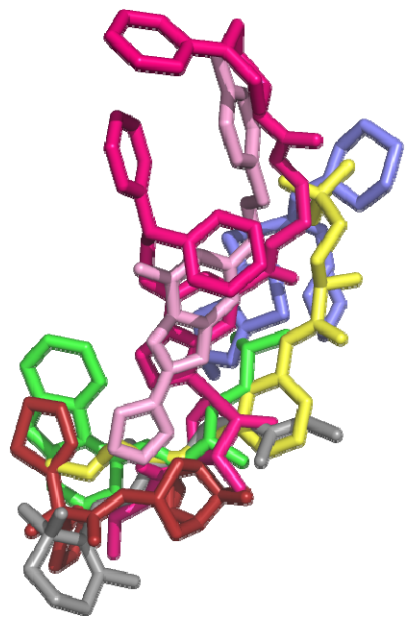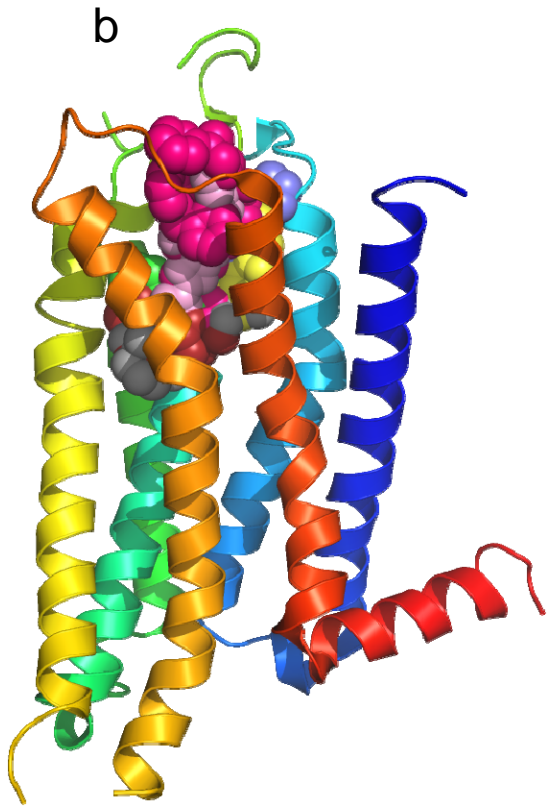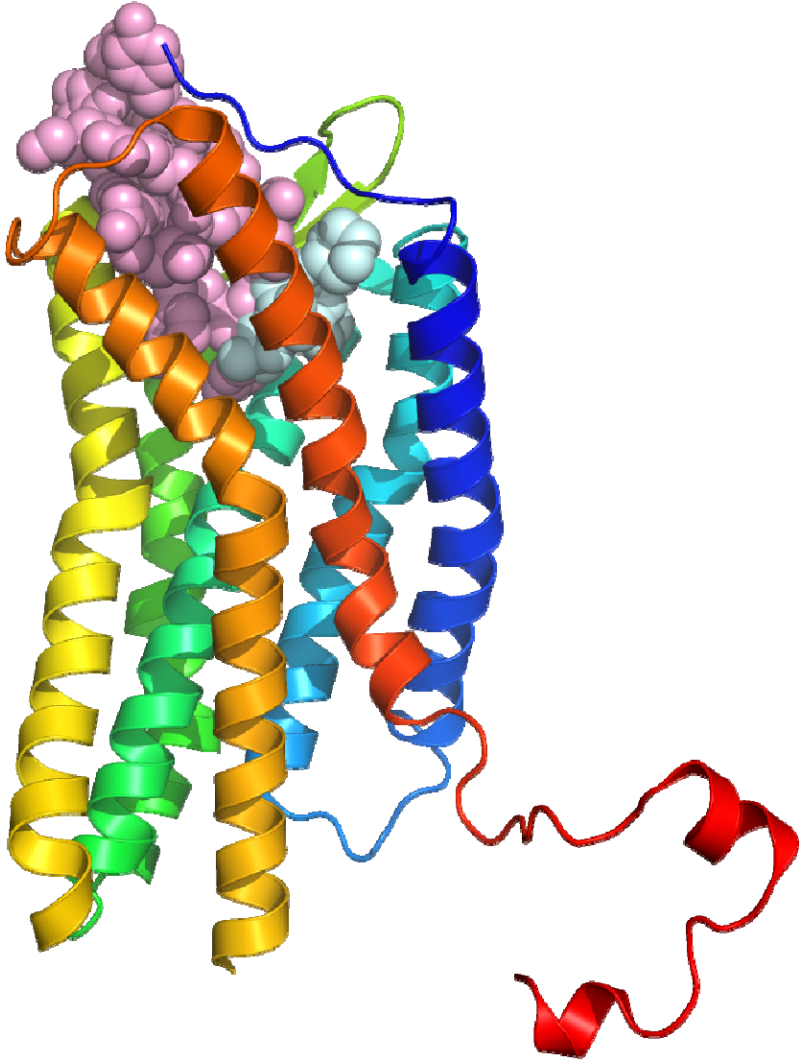
CXCR4

NT

EL2

TM2

TM7

TM3

S1P1

NT

EL2

TM2

TM5

TM7

TM3

TM6

Figure 4

a

b

Figure 5

Figure 6